Evaluation of the preparation and fertilizer release performance of planting concrete made with recycled-concrete aggregates from demolition

Laibo Li[a], Mingxu Chen[a], Xiangming Zhou[b], Lingchao Lu[a,*], Yi Wang[a], Xin Cheng[a,*]

[a] School of Materials Science and Engineering, University of Jinan, Jinan 250022, China

[b] Department of Civil & Environmental Engineering, Brunel University, London, Uxbridge, Middlesex UB8 3PH, United Kingdom

Abstract

This paper developed a new generation of planting concrete (PC) made from recycled aggregates of demolished concrete (RADC) to improve the fertilizer retention properties and reduce the cost. By optimizing the fabrication procedures and mix proportions of the planting concrete with RADC (PC-RADC), the interconnected porosity, water permeability coefficient and 28-day compressive strength can be enhanced to 40.9 %, 2.88 cm/s and 6.5 MPa, respectively, which laid a fundamental basis for the improved release of fertilizer in the developed planting concrete. The experimental results revealed that with the addition of 4.4 kg/m^3 urea fertilizer, not only the 28-day release rate of nitrogen, a key parameter representing the fertilizer release performance, of the PC-RADC was improved by 72.1 %, but also a more stable pore fluid alkalinity at approximately 8.20 pH was developed, which provided a suitable environment for plant growth. Moreover, the frost resistance of the urea fertilized PC-RADC was enhanced by 12.4 % with the reduction of 150-day drying shrinkage rate by 20.5 %. In conclusion, utilization of RADC has a great potential for the sustainable PC development with improved fertilizer release performance.

Key words: Planting concrete (PC); Recycled aggregates from demolished concrete (RADC); Fertilizer release performance.

1. Introduction

Utilization of porous concrete as a substitute for conventional concrete has been rapidly developed towards a sustainable, multifunction and intelligent material to realize the environment protection and sustainable development of modern civil infrastructure. Due to the enormous advantages of porous concrete, such as excellent water permeability, good thermal insulation properties and lightweight nature (Lu et al., 2015, 2018), it not only provides a realistic solution to erosion and flooding caused by impervious land development, but also satisfies the bio-adaptability and plant-growing characteristics of substrate as a planting concrete (PC) (Kim and Lee, 2010; Park and Tia, 2004; Jang et al., 2015; Ćosić et al., 2015), as shown in Fig. 1(a) (Huang et al., 2016; Li et al., 2017a; Lu et al., 2016). It also has been widely applied in permeable trenches, gullies, and gutters (Bhutta et al., 2012), and in noise barriers (Ćosić et al., 2015; Kim and Lee, 2010) etc. In fact, PCis a ecological type of porous concrete, compared with ordinary concrete, it is more efficient to protect water and soil loss on the slopes of river banks and roadbeds (Fig. 1(b)) (Tarnai et al., 2004, 1998) and therefore prevent the soil erosion and desertification (Li et al., 2017a; Yan et al., 2013). Roots of plants could pass through the PC via pores structure to absorb nutrition underground (Fig. 1(c)). However, in order to ensure efficient plant growth in PC, the following issues should be addressed: (1) providing enough spaces for root growth; (2) ensuring the effective retention of fertilizer and (3) reducing the amount of alkali leaching (Li et al., 2017a; Tarnai et al., 2004).

Regarding the issue of providing enough spaces for root growth, Tarnai et al. suggested that the interconnected void ratio of PC should be at least 25 % for immediate growth, 21 % for late growth and 18 % for viable growth (Tarnai et al. 2004). Besides, it also revealed that the addition of coarse aggregates with the range of 15-20, 15-25, 20-25 and 20-30 mm benefited to developing PC with suitable interconnected void ratio. Among various of coarse aggregates, crushed natural resources, including limestone and granite, have been regarded as an excellent candidate to fabricate PC due to its low water absorption rate and crush index et al., but the natural resources crisis has greatly limited its widely application (Taylor et al., 2007; Shi et al., 2016). Therefore, it is of importance to find a sustainable replacement material in large quantities with technical performance comparable to that of existing natural aggregates. Currently, many waste materials have been used to replace natural aggregates, for instance steel slag, copper slag and construction and demolition waste. Among them, construction and demolition waste has been assessed as a reliable source of untapped waste materials with a high valorisation potential and the most significant waste streams in the world, accounting for over 650 million tonnes per year, with waste demolition concrete (WDC) representing 85 % (Silva et al., 2017; João et al., 2017). Therefore, utilization of WDC as recycled-concrete aggregates for producing PC would offset the energy intensive quarrying process of natural aggregates and protect the environment from waste landfill. More importantly, it is very convenient and cost-effective for post-processing (breaking, removing and crushing) of the WDC for recycling aggregates use (Blengini and Garbarino, 2010; Miguel et al., 2015). All the benefits above have driven the WDC as an energy effective materials widely utilized in various applications, such as bulk filling, revetment, roadbeds, base material for drainage structures, noise barriers and embankments (Ajdukiewicz and Kliszczewicz, 2002; Silva et al., 2017). Although extensive research has been conducted to investigate the influence of waste demolition concrete as recycled aggregates on the properties of porous concrete (Ćosić et al., 2015; Lamond et al., 2002; Bhutta et al., 2013;), few of them studied the efficiency of recycled-concrete aggregates from demolition for PC.

Regarding the issue of fertilizer retention of PC, solid or liquid forms of fertilizer should be regularly supplied since nutrients content (e.g. nitrogen and phosphorus) necessary for plant growth is scarce in Portland cement concrete (PCC) (Li et al., 2017a, 2017c). Nitrogen and phosphorus from fertilizers are even more easily lost in PCC based on the theory of 'fertilizer moves with water' (Li et al., 2010; Alberts and Moldenhauer, 1981), indicating that fertilizers should be continually supplied to meet the nutritional demands of plant growth, which is labor-consuming and cost-ineffective. More serious is the high alkalinity (PH=13.5) of PCC due to the formation of C-S-H gel and calcium hydroxide (Kaminskas et al., 2015; Keren et al., 2015), and the alkali leaching plays a negative role for plant growth. To our best knowledge, both of disadvantages above, poor fertilizer retention and alkali leaching， can be mitigated by using sulphoaluminate cement (SAC). Compared with Portland cement, SAC not only has a lower alkalinity value of 11.5 due to the special hydration products, namely ettringite (AFt, $C_3A{\cdot}3C\${\cdot}H_{32}$, where C = CaO, A = Al_2O_3, \$ = SO_3, H = H_2O) and calcium aluminate sulphate hydrate gel (AFm, $C_3A{\cdot}C\${\cdot}H_{12}$) (Martin et al., 2015; Juenger et al., 2011; Chen et al., 2017), which allows it to create a more favourable environment for plant growth, but also has the advantages of a lower calcination temperature (~1250 °C), lower CO_2 emissions and easier grinding with less energy required (Li et al., 2017b; Dong et al., 2014; Chen et al., 2016; García-Maté and Torre, 2013; Berger and Aouad, 2013), which is more energy efficient and sustainable. In addition, SAC also allows for reduced construction time because of the fast setting and high early strength gain (Trauchessec et al., 2015; Liao et al., 2011; Bernardo et al., 2006). More importantly, a number of previous studies (Li et al., 2017a, 2017c; Huang et al., 2016) demonstrated that the release rate of fertilizer in the hardened SAC pastes was much slower than that in Portland cement. Therefore, SAC is an excellent candidate to replace Portland cement for developing PC with improved fertilizer retention.

The objective of this paper is to develop a new generation of PC made from SAC as matrix and recycled waste demolition concrete as coarse aggregates, which is expected to have improved fertilizer retention properties, reduced the cost and satisfied mechanical performance. Firstly, the influence of different consolidation methods and mixing order of raw materials on the properties (e.g. the void ratio, water permeability and compressive strength) of PC was investigated. Secondly, the fertilizer release performance of the developed PC modified by two kind of fertilizers, urea and diammonium phosphate, was evaluated and compared by measuring the release rate of nitrogen. Finally, the effect of fertilizers on the alkalinity, drying shrinkage and frost resistance of PC was studied.

2. Experimental Procedures

2.1 Materials

SAC (Grade 42.5 R according to Chinese National Standards GB20472-2006, manufactured in Special Cement Co., Ltd of Qufu, China) was used as the binder to fabricate the PC. The chemical composition of the SAC was analyzed by an X-ray fluorescence spectrometer (XRF, Tiger S8, Germany), as listed in Table 1. X-ray diffraction (XRD) and quantitative X-ray diffraction (QXRD) were employed to measure and quantify the main phases of SAC, the results of which are shown in Fig. 2 and Table 2. Crushed limestone rubble and waste demolition concrete were used as the natural and recycled coarse aggregates, respectively. The physical properties of both aggregates are represented in Table 3. Fig. 3 shows the lab-based crushing process for the waste demolition concrete.

Urea ($CO(NH_2)_2$, purity of 99.0 wt. %, Sinopharm Chemical Reagent Co., Ltd, China) and diammonium phosphate (DP, $(NH_4)_2HPO_4$, purity of 99.0 wt. %, Sinopharm Chemical Reagent Co., Ltd, China) were used as the two fertilizers in this study. Boric acid (BA, purity of 99.0 wt. %, Sinopharm Chemical Reagent Co., Ltd, China) along with polycarboxylate polymer (PP, Shandong Academy of Building Research, China) were incorporated into the PC as the retarder and superplasticizer, respectively.

2.2 Experimental

2.2.1 Sample Preparation

Details on the mix proportions and preparation methods of PC are listed in Table 4. SAC was mixed with double distilled H_2O at the water/cement (*w/c*) ratio of 0.25 (Jang et al., 2015). The weight ratios of aggregate/cement, BA/cement and PP/cement were fixed at 6.000, 0.004 and 0.011for all mixes.

Three methods (A, B and C) with different mix order were used to fabricate PC in this study, as shown in Table 5, followed by three different consolidation methods. Fresh mixture was cast into cylindrical molds (φ-100 mm × 200 mm) and cube molds (100× 100× 100 mm), and then consolidated by the following three ways: (1) vibration (V, 3 -15 s), (2) pressure (P, 0.5 - 2.0 MPa) or (3) ramming (R). Specimens were then cured at a temperature of 20 ± 2 ºC and humidity of 95+ 5 % RH. After 24 hours, specimens were demolded and placed back for further curing under the same conditions until further testing.

2.2.2 Fertilizer Release Performance

Based on the optimum preparation method obtained from the section of 2.2.1, urea and DP were then individually added to the PC, based on the mix proportions listed in Table 6. The cubic specimens (100× 100× 100 mm) were used to measure the compressive strength, fertilizer release rate and alkalinity of pore fluid of the fertilized PC. Two types of beam specimens (100× 100× 515 mm and 100×100×400 mm) were prepared for measuring the drying shrinkage rate and frost resistance. Finally, cylinder specimens (φ-100× 200 mm) were prepared for void ratio and water permeability tests. All specimens were cured in the exact same conditions as described in the section of 2.2.1.

2.3 Measurements

2.3.1 Void Ratio Test

The total void ratio (R_{TV}) was obtained according to the following equation:

$$R_{TV} = \left[1 - \frac{M_2 - M_1}{\rho_W \mathrm{V}}\right] \times 100\%$$

where (M_1) is the initial mass of the cylinder samples in the water, (M_2) is the final mass tested following air drying (25±1 ºC, 20±2% RH) for 24 hours, (V) is the sample volume and (ρ_W) is the density of water.

Similarly, the connected void ratio (R_{CV}) was obtained according to the following equation:

$$R_{CV} = \left[1 - \frac{M_3 - M_1}{\rho_W \mathrm{V}}\right] \times 100\%$$

where (M_3) is the final mass measured following air curing (25±1 ºC, 95±2% RH) for 24 hours.

2.3.2 Coefficient of Water Permeability (CWP)

The CWP of planting concrete was measured in accordance with (ISO 17785-1, 2016; Tarnai et al., 2004; Shen et al., 2013), for which the experimental set-up is shown in Fig. 4. The CWP was determined over a period of 50 seconds under a water head of 150 mm and calculated according to the following equation:

$$K_r = \frac{\mathrm{H}}{\mathrm{h}} \times \frac{\mathrm{Q}}{\mathrm{A}(t_2 - t_1)}$$

where Kr is the CWP (cm/s), H is the specimen length (cm), Q is the volume of water discharge from t_1 to t_2 (cm^3), h is the difference of water head, t_2-t_1 is time (s) and A is the cross sectional area of the cylindrical specimen (cm^2).

2.3.3 Compressive Strength

For compressive strength test, three capped cubic specimens were tested at a loading rate of 2 mm/min by a 2000 KN capacity hydraulic testing device (DC-2000, China), according to the Chinese National Standard GB 50081-2002 (GB/T 50081, 2002).

2.3.4 Fertilizer Release Rate and Alkalinity of Pore Fluid

The fertilizer release rate can be divided into two parts: a nitrogen release rate and a phosphorus release rate. Samples were soaked in a container with 10 L deionized water (Fig. 5) at a temperature of 20 ± 1 ºC. At the age of 1 day, 3 days, 7 days and 28 days, the nitrogen and phosphorus concentration of the soaking solution were measured according to the Chinese National Standards GB 11894-1989 (GB/T 11894, 1989) and GB 11893-1989 (GB/T 11893, 1989), respectively. Correspondingly, pH value of the soaking solution was measured using a laboratory grade pH meter (pHs-3E, China). It should be noted that after every single test, the container was re-filled with 10 L pure deionized water to avoid the saturation effect.

2.3.5 Drying Shrinkage

The drying shrinkage was determined according to the Chinese National Standard GB 50082-2009 (GB/T 50082, 2009), the set-up of which is shown in Fig. 6. Specimens for the drying shrinkage were cured at 20 ± 2 ºC and 95+% RH for 3 days. After that, testing specimens were cured at a temperature of 20 ± 1 ºC and humidity of 65 ± 5% RH. The length of the specimen was accurately measured at the predetermined times of 1 day, 3 days, 5 days, 7 days, 10 days, 14 days, 20 days, 28 days, 45 days, 60 days, 90 days and 150 days and the drying shrinkage was calculated based on the following equation:

$$\varepsilon = \frac{L_0 - L_t}{L_0}$$

where (ε) is the drying shrinkage rate, L_0 is the initial beam length and L_t is the final beam length.

2.3.6 Frost Resistance

Frost resistance test was carried out according to the Chinese National Standard GB 50082-2009 (GB/T 50082, 2009). The schematic view of frost resistance is shown in Fig. 7. Test samples (100 mm × 100 mm × 400 mm) were prepared according to the fast freeze-thawing method and were cured as standard for 2 days followed by insertion in 20±1 ºC deionized water for 24 hours. The samples were subsequently taken out from deionized water, surface dried, accurately weighed and recorded as m_0. A total of 40 freeze-thaw cycles implemented, where one cycle consisted of freezing at -18 ºC for 4 hours and thawing at 18 ºC for 2 hours. Samples were then accurately weighted and recorded as m_1. The weight loss rate (WLR) of the sample was used as a parameter to reflect the frost resistance of planting concrete and calculated using the following equation:

$$\mathrm{WLR} = \frac{m_0 - m_1}{m_0} \times 100\%$$

3. Results and Discussion

3.1 Effect of Vibration Time on the Basic Properties of PC

Fig. 8 shows the void ratio and CWP of PC mixed by Method A and consolidated by vibration. In terms of void ratio, it is clear to see that the total and interconnected void ratios of PC decrease with the increasing vibration time, as shown in Fig. 8a. For example, the control sample *Aref* (without any consolidation) shows the highest total and interconnected void ratio at 47.1 % and 43.4 %, which are approximately equal to the void ratio of recycled aggregate stacking (48.4%, Table 3). It indicates that the stacking of aggregates is not compact if the PC is prepared without any consolidation. At the longest vibration time of 25 seconds i.e. sample AV5, the total void and interconnected void ratio of PC sharply decrease to 41.3 % and 36.5 %, respectively. A similar trend can also be found in the CWP of PC, as shown in Fig. 8b. Previous studies (Neithalath et al., 2010; Bhutta et al., 2013) demonstrated that there was a linear correlation between the void ratio and CWP of the ordinary pervious concrete. Therefore, the relationship between the interconnected void ratio and CWP of planting concrete can be established, as shown in Fig. 9. The correlation coefficient between the interconnected void ratio and CWP reaches up to 0.92, confirming that there is an extremely significant linear correlation between the two parameters similar to the ordinary pervious concrete. It also suggesting that the CWP of PC made with recycled aggregates depends on its interconnected void ratio.

It is shown in Fig. 10 that the compressive strength of every vibrated PC is higher than that of the un-vibrated PC. Maximum values at 1 day, 3 days and 28 days reach up to 3.9, 5.1 and 8.5 MPa, respectively, for the PC with a vibration time of 15 seconds. More importantly, Fig. 11 shows the correlation between the total void ratio and compressive strength of PC. Fig.11a reveals a strong correlation up to the vibration time of 15 seconds, while vibration time long than that leads to a decrease in the correlation coefficient between the total void ratio and compressive strength, as shown in Fig. 11b. This phenomenon can be explained by that the recycled aggregates which loosely stack before vibration turn more compact with the increasing vibration time. However, with more than 15 seconds of vibration, the SAC paste is more likely to detach from the aggregates and precipitate to the bottom of PC mixture, as shown in Fig. 12, leading to a significant reduction of SAC paste as the binder in PC.

3.2 Effect of Pressure on the Properties of PC

Fig. 13 shows the void ratio and CWP of PC mixed by Method A and consolidated by pressure. It evidently shows that both parameters of PC decrease with the increase of consolidation pressure. When the pressure reached 1.0 MPa i.e. sample *AP2*, the interconnected and total void ratios of PC decrease by 12.9 % and 10.6 %, respectively. As shown in Fig. 14, for this consolidation method, the correlation coefficient of interconnected void ratio and CWP of PC is 0.99, suggesting that there is a strong linear correlation between the two parameters. It also confirms the conclusion that the water permeability of PC depends on its interconnected void ratio.

Fig. 15 presents the effect of consolidating pressure on the compressive strength of PC. The results indicate that the highest 1-, 3- and 28-day compressive strengths are up to 2.8, 4.9 and 6.3 MPa, respectively, at the consolidation pressure of 1.0 MPa. Following the correlation relationship between the total void ratio and compressive strength of PC (consolidated by pressure) (Fig. 16), it can be observed that the correlation coefficient up to the pressure of 1.0 MPa significantly increases, as shown in Fig. 16a. However, when the consolidation pressure increases further to 2.0 MPa, the correlation coefficient greatly decreases with the increase of consolidation pressure (Fig. 16b). The loss of compressive strength and correlation coefficient can be explained by the difference in recycled concrete aggregate composition compared to natural stone aggregates. The recycled concrete aggregate contains two additional components, namely, adhered mortar and an interfacial transition zone (ITZ) between the natural aggregate and the original cement mortar (Shi et al., 2016). Therefore, the bonding between cement paste and recycled aggregate is weaker than between cement paste and natural aggregate (Bhutta et al., 2013). In addition, ITZ is considered to be the weakest region of the recycled concrete aggregate due to the existence of numerous cracks and porosity (Zhang et al., 2015). The weakness of the ITZ can also be reflected from the value of crushing index listed in Table 3, indicating that the crushing index value of recycled concrete aggregates (18.3%) is twice as much as that of natural aggregates (9.3 %) and the.

3.3 Effect of Mixing and Consolidating Methods on the Basic Properties of PC

Fig. 17 shows the interconnected void ratio and CWP of PC prepared by different mixing and consolidating methods. For mixing Method A, it is clear to see that the interconnected void ratio and CWP of the concrete without any consolidation i.e. sample *A ref* （Fig. 8）, are the highest among all the mixing methods. In addition, the interconnected void ratio of the PC consolidated by ramming (sample *AR*) is higher than that of the PC consolidated by vibrating for 15 seconds (sample *AV3*) and by pressure for 1.0 MPa (sample *AP2*), while the CWP of sample *AR* is slightly lower than that of sample *AP2*. Furthermore, the 1-, 3- and 28-day compressive strength of sample *AR* is obviously higher than that of sample *AV3* and sample *AP2*. Therefore, based on the mixing Method A, PC consolidated by ramming shows the optimum properties. For mixing Method B, the interconnected void ratio and CWP of PC consolidated by pressure at 1.0 MPa (sample *BP2*) is obviously higher than that of the concrete consolidated by vibrating for 15 seconds (sample *BV3*) and by ramming (sample *BR*), and the 1- and 3-day compressive strength of sample *BP2* is similar to that of sample *BV3* and sample *BR*. So, based on the mixing Method B, PC consolidated by pressure at 1.0 MPa showed the optimum properties. For mixing Method C, the interconnected void ratio and CWP of PC consolidated by pressure at 1.0 MPa (sample *CP2*) is obviously higher than that of the PC consolidated by vibrating for 15 seconds (sample *CV3*) and by ramming (sample *CR*), and the 1-, 3- and 28-day compressive strength of sample *CP2* is similar to that of sample *CV3* and sample *CR*. Hence, based on the mixing Method C, PC consolidated by pressure at 1.0 MPa shows the optimum properties. In sample *AR*, sample *BP2* and sample *CP2*, by contrast, the interconnected void ratio of sample *AR* is similar to that of sample *BP2* and sample *CP2*, and the CWP and 1-, 3- and 28-day compressive strength of sample *AR* is obviously higher than that of sample *BP2* and sample *CP2*. In summary, mixing procedure A and consolidation by ramming i.e. sample *AR* show the optimum properties, namely, an interconnected void ratio of 40.9 %, a CWP of 2.88 cm/s and a 28-day compressive strength of up to 9.5 MPa. In summary, mixing procedure A and consolidation by ramming will be used to prepare PC samples for testing fertilizer release performance, alkalinity, shrinkage and frost resistance.

3.4 Fertilizer Release Performance

The released amount and cumulative release rate of nitrogen are the two parameters representing the fertilizer release performance of PC. Fig. 19 shows the release amounts and cumulative release rates of nitrogen of planting concrete with urea.. It is evident that the cumulative release rate of nitrogen increases for all samples with the increase of soaking time. Nonetheless for sample *RU1*, the cumulative release rate of nitrogen is only 25.0 % at 28 days, suggesting that the urea is slowly released from the hardened PC if it is added during the mixing process of raw materials. The decreased release rate of urea partly results from its absorption by aggregates due to the 'fertilizer moves with water' theory (Li et al., 2017a), and the rest of urea is distributed in the hardened SAC paste. Since the total porosity of the hardened SAC paste can reach 0.09 cm^3/g (Li et al., 2017b) and the void ratio for PC is about 40 %, the urea could move from recycled aggregate and hardened paste to water. So, the nitrogen could dissolve out from hardened PC after the concrete is kept in deionized water. An additional phenomenon worth noting is that the release amount and cumulative release rate of nitrogen increase with the increase of urea addition at the same soaking time. For instance, when the urea dosage is 0.44 kg/m^3 (sample *RU1*), 4.4 kg/m^3 (sample *RU2*) and 7.7 (sample *RU3*) kg/m^3, the release amounts of nitrogen for 1 day is 7.9 mg/L, 481.6 mg/L and 1017.3 mg/L and the release amounts of nitrogen for 28 days is 17.7 mg/L, 394.6 mg/L and 571.5 mg/L, respectively. It might result from that the concentration gradient of nitrogen between inside and outside of the concrete increases with the increase of urea dosages and the release speed increases with the increase of concentration gradients.

Fig. 20 and Fig. 21 show the released amount and cumulative release rate of nitrogen and phosphorus of PC with DP. The release amounts of nitrogen and phosphorus increases with the increasing amount of DP at the same soaking time. In addition, the cumulative release rate of nitrogen and phosphorus increase with the increase of soaking time and the DP addition at same soaking time. However, the 28-day cumulative release rate of nitrogen of PC with 0.44 kg/m^3 DP (sample *RD1*), 4.4 kg/m^3 DP (sample *RD2*) and 7.7 kg/m^3 DP (sample *RD3*) reaches up to 16.11 %, 45.43 % and 66.75 %, respectively, and the cumulative release rate of phosphorus of sample *RD1*, sample *RD2* and sample *RD3* for 28 days is only 0.007 %, 0.030 % and 0.033 %, respectively. This phenomenon suggests that the nitrogen could easily dissolve out from the hardened PC after the concrete is kept in deionized water, while the phosphorus is difficult to dissolve out. The mechanism behind can be described as below: DP could hydrolyze to NH_4^+ and HPO_4^{2-} ($(NH_4)_2HPO_4 \rightarrow 2NH_4^+ + HPO_4^{2-}$) and the latter one could further hydrolyze to H^+ and PO_4^{3-} ($HPO_4^{2-} \rightarrow H^+ + PO_4^{3-}$) (Kumar and Behal, 2017; Shah et al., 2016), which can react with divalent cations (Ca^{2+},

Mg^{2+}) to produce insoluble phosphate ($CaHPO_4$, $Ca_3(PO_4)_2$, Mg_3HPO_4 and $Mg_3(PO_4)_2$) (Kokubo et al., 1991; Kjellin et al., 2016; Castro et al. 2017). Therefore, the cumulative release rate of phosphorus is much lower than that of nitrogen, and that is the reason why it is difficult for plants to absorb phosphorus from PC with DP and therefore extra supply of phosphate fertilizer is required for plants growth.

3.5 Alkalinity

Fig. 22 shows the pH value of the pore solution in PC. From Fig. 22a, it can be seen that the alkalinity of PC prepared with recycled aggregates (sample *Rref*) is lower than that of the concrete prepared by natural aggregate (sample *N*). This is mainly due to the unit weight of natural aggregates being higher than that of recycled aggregates under the same weight ratio of aggregate-to-cement (Table 3). So, the amount of SAC used in samples *N* (265 kg/m^3) is higher than that used in sample *Rref* (220 kg/m^3) (Table 6). The result confirms that the recycled concrete aggregates are suitable in the preparation of PC due to its lower density. The PH value of the pore fluid in sample *RU1, RU2 and RU3* is 8.29, 8.23 and 8.24 at 28 days, respectively which is similar to that of sample *Rref*. However, the alkalinity of the pore fluid of PC increases with the increase of DP addition. When the DP dosage reaches to 7.7 kg/m^3 (sample *RD3*), the 28-day alkalinity of the pore fluid in sample *RD3* is increased by 14.8 % to a value of 9.38. The most likely reason is that DP could react with CH to form insoluble phosphate ($CaHPO_4$ and $Ca_3(PO_4)_2$) and ammonium hydroxide (AH; $NH_3{\cdot}H_2O$), which easily transforms into $NH_4^+$and OH^- ($NH_3{\cdot}H_2O \rightarrow NH_4^+ + OH^-$), leading to the increased alkalinity. Therefore, it can be concluded that DP is not suitableto prepare fertilized PC.

3.6 Drying Shrinkage

Fig. 23 displays the drying shrinkage of PC fertilized with Urea and DP. It indicates that the drying shrinkage of PC increases with the increasing of curing time. When the curing time is up to 150 days, the drying shrinkage rate of sample *Rref* is 147.1×10^{-6}, which is higher than that of sample *N* (i.e. 117.7×10^{-6}). Generally, the drying shrinkage of concrete occurs when the free water stored in the capillary pores evaporates due to a low relative-humidity environment. This circumstance leads to a humidity gradient which induces the transport of water particles from the gel to the capillary pores after which it evaporates (Gonzalez-Corominas and Etxeberria, 2016). Since drying shrinkage can generate internal stress, mass loss and consequently volume reduction of the PC, the amount of water evaporation from the PC prepared with recycled aggregates is therefore higher than that of the PC prepared with natural aggregates due to the water absorption of the recycled aggregates being much higher than that of natural aggregate (Table 3). More importantly, the addition of Urea can effectively reduce the drying shrinkage rate of PC prepared with recycled aggregates. The experimental results indicate that the dry shrinkage rate of sample *RU2* is only 117.0×10^{-6} at 150 days, which is comparably close to the value obtained from sample *N*. The reduced drying shrinkage is attributed to the formation of AFm (Huang et al., 2016). With the help of Urea, AFt generated in the SAC hydration could be transformed to AFm, which shows a better stability in the drying condition (Li et al., 2017c; Huang et al., 2016). However, DP could increase the drying shrinkage rate of PC prepared with recycled aggregates. The dry shrinkage rate of sample *RD2* rises to 176.5×10^{-6} at 150 days. Hence, urea is more suitable than DP in the preparation of PC using recycled aggregates.

3.7 Frost Resistance Property

Fig. 24 shows the frost resistance of PC from a qualitative point of view. The mass loss rate of PC increases with the increase of freezing and thawing cycles. When the number of cycles reaches to 40, the mass loss rate of sample *Rref* is 3.77%. At the same time, the mass loss rate of sample *N* is only 2.73%. This result confirms that the frost resistance of PC prepared by recycled concrete aggregates is worse than the concrete prepared by natural aggregates. The likely reason is that the inherent frost resistance of recycled aggregates is much lower than that of natural aggregates (Fig. 24b) due to its high water absorption (Table 3). Therefore, the mass loss rate of the PC prepared with recycled aggregates is higher than that of the PC prepared with natural aggregates. Furthermore, addition of urea improves the frost resistance of planting concrete using recycled aggregates while DP has a counteractive effect. It might result fromfrom the fact that urea is beneficial to the hydration and hardening of SAC (Huang et al., 2016), while DP could react with CH to form insoluble phosphate ($CaHPO_4$ and $Ca_3(PO_4)_2$) with unsatisfactory cementitious properties (Steink et al., 1991), which is negative to SAC hardening.

4. Conclusions

Recycled aggregates from demolished concrete (RADC) was adopted to prepare a new generation of planting concrete (PC) with enhanced fertilizer release performance. The preparation methods, fertilizer release performance, alkalinity, dry shrinkage and frost resistance of the PC were investigated in the current study. The investigation supports the following conclusions:

(1) RADC was suitable for developing the PC with improved fertilizer release performance. By optimizing the fabrication procedures (i.e. mixing procedure A: 1) Recycled aggregates and water were mixed together in a concrete mixer for 30 seconds; 2) SAC was slowly added into the mixture in 60 seconds; 3) The fresh mixture was further mixed for another 60 seconds and consolidation by ramming) and mix proportions, the interconnected porosity, water permeability coefficient and 28-day compressive strength of the PC with 4.4 kg/m^3 addition of RADC can be increased to 40.9 %, 2.88 cm/s and 6.5 MPa, respectively.

(2) A novel PC fertilized with urea showed improved nitrogen and release rate. Using a urea addition of 4.4 kg/m^3, the cumulative release rate of nitrogen at 28 days of PC reached up to 72.1 %.

(3) A novel PC modified by RADC showed a stable pore fluid alkaline environment at approximately 8.20 pH, which was more suitable for plant growing.

(4) With the addition of urea, the frost resistance of planting concrete can be improved by 12.4 % with the reduction of 150-day drying shrinkage rate by 20.5 %. In contrast, the addition of DP resulted in a greater mass loss rate and was not be recommended for use as a fertilizer in PC.

Acknowledgments

This work is supported by the National Key Point Research and Invention Program of the Thirteenth through the grants of NO.2016YFC0701000, the National Natural Science Foundation of China through the grants of NO.51472109 and NO.51302104, and Science and Technology Development Plan of Shandong Province through the grant of NO.2014GZX208001. In addition, this work is also supported by the Program for Scientific Research Innovation Team in Colleges and Universities of Shandong Province.

Reference

Ajdukiewicz, A., Kliszczewicz, A., 2002. Influence of recycled aggregates on mechanical properties of HS/HPC. Cem. Concr. Comp. 24(2), 269-279. https://doi.org/10.1016/S0958-9465(01)00012-9

Alberts, E.E., Moldenhauer, W.C., 1981. Nitrogen and phosphorus transported by eroded soil aggregates. Soil Sci. Soc. Am. J. 45 (2), 391-396. https://doi.org/10.2136/sssaj1981.03615995004500020032x

Berger, S., Aouad, G., 2013. Leaching of calcium sulfoaluminate cement pastes by water at regulated pH and temperature: experimental investigation and modeling. Cem. Concr. Res. 53, 211-220. https://doi.org/10.1016/j.cemconres.2013.06.014

Bernardo, G., Telesca, A., Valenti, G. L., 2006. A porosimetric study of calcium sulfoaluminate cement pastes cured at early ages. Cem. Concr. Res. 36, 1042-1047. https://doi.org/10.1016/j.cemconres.2006.02.014

Bhutta, M.A.R., Tsuruta, K., Mirza, J., 2012. Evaluation of high-performance porous concrete properties. Constr. Build. Mater. 31 (6), 67-73. https://doi.org/10.1016/j.conbuildmat.2011.12.024

Bhutta, M.A.R., Hasanah, N., Farhayu, N., et al., 2013. Properties of porous concrete from waste crushed concrete (recycled aggregate). Constr. Build. Mater. 47, 1243-1248. http://dx.doi.org/10.1016/j.conbuildmat.2013.06.022

Blengini, G.A, Garbarino, E., 2010. Resources and waste management in Turin (Italy): the role of recycled aggregates in the sustainable supply mix. J. Clean. Prod. 18(10-11), 1021-1030.

https://doi.org/10.1016/j.jclepro.2010.01.027

Castro, A.G.B., Polini, A., Azami, Z., et al., 2017. Incorporation of PLLA micro-fillers for mechanical reinforcement of calcium-phosphate cement. J. Mech. Behave. Biomed. 71, 286-294. https://doi.org/10.1016/j.jmbbm.2017.03.027

Chung S., Han T., Kim S., Lee T., 2014. Investigation of the permeability of porous concrete reconstructed using probabilistic description methods. Constr. Build. Mater. 66, 760-770. http://dx.doi.org/10.1016/j.conbuildmat.2014.06.013

Chen M., Wang S., Lu L., et al., 2016. Effect of matrix components with low thermal conductivity and density on performances of cement-EPS/VM insulation mortar. J. Therm. Anal. Calorim. 126 (3), 1123-1132. https://doi.org/10.1007/s10973-016-5718-x

Chen M., Lu L., Wang S., et al., 2017. Investigation on the formation of tobermorite in calcium silicate board and its influence factors under autoclaved curing. Constr. Build. Mater. 143, 280-288. https://doi.org/10.1016/j.conbuildmat.2017.03.143

Ćosić, K., Korat, L., Ducman, V., Netinger, I., 2015. Influence of aggregate type and size on properties of pervious concrete. Constr. Build. Mater. 78, 69-76. https://doi.org/10.1016/j.conbuildmat.2014.12.073

Dong, X., Wang, S., Gong, C., Lu, L., 2014. Effects of aggregate gradation and polymer modifyers on properties of cement-EPS/ vitrified microsphere mortar. Constr. Build. Mater. 73, 255-260. https://doi.org/10.1016/j.conbuildmat.2014.09.064

García-Maté, M., Torre, A. G. D., 2013. Hydration studies of calcium sulfoaluminate cements blended with fly ash. Cem. Concr. Res. 54, 12-20. https://doi.org/10.1016/j.cemconres.2013.07.010

GB, GB/T 11893, 1989. Water quality-Determination of total phosphorus-Ammonium molybdate spectrophotometric method. Standardization Administration of the People's Republic of China, Beijing, China. (in Chinese)

GB, GB/T 11894, 1989. Water quality-Determination of total nitrogen-Alkaline potassium persulfate digestion-UV spectrophotometric method. Standardization Administration of the People's Republic of China, Beijing, China. (in Chinese)

GB, GB/T 20472, 2006. Sulphoaluminate cement. Standardization Administration of the People's Republic of China, Beijing, China. (in Chinese)

GB, GB/T 50081, 2002. Standard for test method of mechanical properties on ordinary concrete. Standardization Administration of the People's Republic of China, Beijing, China. (in Chinese)

GB, GB/T 50082, 2009. Standard for test method of long-term performance and durability of ordinary concrete. Standardization Administration of the People's Republic of China, Beijing, China. (in Chinese)

Gonzalez-Corominas, A., Etxeberria, M., 2016. Effects of using recycled concrete aggregates on the shrinkage of high performance concrete. Constr. Build. Mater. 115, 32-41. http://dx.doi.org/10.1016/j.conbuildmat.2016.04.031

Hu, J., Wang, Z., Kim, Y., 2013. Feasibility study of using fine recycled concrete aggregate in producing self-consolidation concrete. J. Sus. Cem. Mater. 2(1), 20-34. http://dx.doi.org/10.1080/21650373.2012.757832

Huang, Q., Zhou, X., Zhuang, L., et al., 2016. Effects of carbamide on sulfoaluminate cement paste for growing plants. Constr. Build. Mater. 113, 229-236. https://doi.org/10.1016/j.conbuildmat.2016.03.003

ISO 17785-1, 2016. Testing methods for pervious concrete-Part 1: Infiltration rate. International Standards Organization.

Jang, J.G., Ahn, Y.B., Souri, H., et al., 2015. A novel eco-friendly porous concrete fabricated with coal ash and geopolymeric binder: Heavy metal leaching characteristics and compressive strength. Constr. Build. Mater. 79, 173-181. https://doi.org/10.1016/j.conbuildmat.2015.01.058

João, P., Jorge, D.B., João, F., Diogo, S., 2017. Dynamic characterization of full-scale structures made with recycled coarse aggregates. J. Clean. Prod. 142, 4195-4205. http://dx.doi.org/10.1016/j.jclepro.2015.08.045

Juenger, M., Winnefeld, F., Provis, J., Ideker, J., 2011. Advances in alternative cementitious binders. Cem. Concr. Res. 41, 1232-1243. https://doi.org/10.1016/j.cemconres.2010.11.012

Kaminskas, R., Cesnauskas, V., Kubiliute, R. 2015. Influence of different artificial additives on Portland cement hydration and hardening. Constr. Build. Mater. 95, 537-544. http://dx.doi.org/10.1016/j.conbuildmat.2015.07.113

Keren, Z., Jin, Z., Mulbah, G., 2015. Influences of phosphate tailings on hydration and properties of Portland cement. Constr. Build. Mater. 98, 593-601. https://doi.org/10.1016/j.conbuildmat.2015.08.115

Kim, H.K., Lee, H. K., 2010. Acoustic absorption modeling of porous concrete considering the gradation and shape of aggregates and void ratio. J. Sound. Vib. 329 (7), 866-879. https://doi.org/10.1016/j.jsv.2009.10.013

Kjellin, P., Rajasekharan, A.K., Currie, F., Handa, P., 2016. Investigation of calcium phosphate formation from calcium propionate and triethyl phosphate. Ceram. Int. 42, 14061-14065. https://doi.org/10.1016/j.ceramint.2016.06.013

Kokubo, T., Yoshihara, S., Nishimura, N, Yamamuro, T, Nakamura, T, 1991. Bioactive bone cement based on CaO-SiO_2-P_2O_5 glass. J. Am. Ceram. Soc. 74 (7), 1739-1741.

https://doi.org/10.1111/j.1151-2916.1991.tb07176.x

Kumar, H., Behal, I., 2017. Volumetric and ultrasonic properties of α-amino acids (glycine, L-alanineand L-valine) in aqueous diammonium hydrogen phosphate at different temperatures and concentrations. J. Mol. Liq. 241, 751-763. https://doi.org/10.1016/j.molliq.2017.06.044

Lamond, J.F., Sr, R.L.C., Campbell, T.R., et al., 2002. Removal and reuse of hardened concrete. ACI Mater. J. 99 (3), 300-325.

Li, X., Zhang, Z., Yang, J., Zhang, G., Wang, B., 2010. Study on the nutrition loss in subsurface runoff under different ecological measures on red soil slope. J. Water Res. & Water Eng. 21 (2), 83-86. (in Chinese)

Li, L., Zhou, X., Li, Y., et al., 2017a. Water absorption and water/fertilizer retention performance of vermiculite modified sulphoaluminate cementitious materials. Constr. Build. Mater. 137, 224-233. https://doi.org/10.1016/j.conbuildmat.2017.01.061

Li, L., Gong C., Wang S., Lu, L., 2017b. Effect of natural zeolite on performance of sulfoaluminate cement-based planting cementitious material. J. Wuhan Univ. Technol. 32 (3), 586-590. https://doi.org/10.1007/s11595-017-1638-2

Li, L., Chen, M., Zhou, X., et al., 2017c. A case of water absorption and water/fertilizer retention performance of super absorbent polymer modified sulphoaluminate cementitious materials. Constr. Build. Mater. 150, 538-546. https://doi.org/10.1016/j.conbuildmat.2017.05.219

Liao, Y., Wei, X., Li, G., 2011. Early hydration of calcium sulfoaluminate cement through electrical resistivity measurement and microstructure investigations. Constr. Build. Mater. 25, 1572-1579. https://doi.org/10.1016/j.conbuildmat.2010.09.042

Lu, Z., Zhang, J., et al., 2015. Effects of the form-stable expanded perlite/paraffin composite on cement manufactured by extrusion technique. Energy. 82, 43-53. https://doi.org/10.1016/j.energy.2014.12.043

Lu, Z., Hanif, A., et al., 2018. A novel lightweight cementitious composite with enhanced thermal insulation and mechanical properties by extrusion technique. Constr. Build. Mater. 163, 446-449. https://doi.org/10.1016/j.conbuildmat.2017.12.130

Lu, Z., Wang, Q., et al., 2016. A novel TiO_2/foam cement composite with enhanced photodegradation of methyl blue. Constr. Build. Mater. 129, 159-162. https://doi.org/10.1016/j.conbuildmat.2016.10.105

Martin, L.H.J., Winnefeld, F., Müller, C.J., Lothenbach, B., 2015. Contribution of limestone to the hydration of calcium sulfoaluminate cement. Cem. Concr. Comp. 62, 204-211. https://doi.org/10.1016/j.cemconcomp.2015.07.005

Miguel, B., Jorge, de B., Jorge, P., Luís, E., 2015. Mechanical performance of concrete made with aggregates from construction and demolition waste recycling plants. J. Clean. Prod. 99, 59-74. http://dx.doi.org/10.1016/j.jclepro.2015.03.012

Neithalath, N., Sumanasooriya, M. S., Deo, O., 2010. Characterizing pore volume, sizes, and connectivity in pervious concretes for permeability prediction. Mater Charact. 61, 802-813. https://doi.org/10.1016/j.matchar.2010.05.004

Park, S.B., Tia, M., 2004. An experimental study on the water-purification properties of porous concrete. Cem. Concr. Res. 34 (2), 177-184. https://doi.org/10.1016/S0008-8846(03)00223-0

Shah, S.H., Raja, I.A., Mahmood, Q., Pervez, A., 2016. Improvement in lipids extraction processes for biodiesel production from wet microalgal pellets grown on diammonium phosphate and sodium bicarbonate combinations. Bioresource Technol. 214, 199-209. https://doi.org/10.1016/j.biortech.2016.04.036

Shen, W., Shan, L., Zhang, T., et al., 2013. Investigation on polymer-rubber aggregate modified porous concrete. Constr. Build. Mater. 38, 667-674. https://doi.org/10.1016/j.conbuildmat.2012.09.006

Shi C, Li Y, Zhang J, et al., 2016. Performance enhancement of recycled concrete aggregate – A review. J. Clean. Prod. 112(1), 466-472. https://doi.org/10.1016/j.jclepro.2015.08.057

Silva, R.V., Brito, J.D., Dhir, R.K., 2017. Availability and processing of recycled aggregates within the construction and demolition supply chain: A review. J. Clean. Prod. 143, 598-614. http://dx.doi.org/10.1016/j.jclepro.2016.12.070

Steink, RA, Silsbe, MR, Agrawal, DK, Roy, R, Roy, DM., 1991. Development of chemically bonded ceramics in the CaO-SiO_2-P_2O_5-H_2O system. Cem. Concr. Res. 21 (1) , 66-72. https://doi.org/10.1016/0008-8846(91)90032-D

Tarnai, M., Mizuguchi, H., et al., 2004. Design, construction and recent applications of porous concrete in Japan. In: Proceedings of the JCI symposium on design, construction and recent applications of porous concrete. Japan Concrete Institute, Tokyo, April. pp: 1-10.

Tarnai, M., Matsukawa, T., 1998. Properties and application of environmentally friendly porous concrete. ACI SP179. pp: 123-140.

Taylor, P.C., Kosmatka, S.H., Voigt, G.F., 2006. Integrated materials and construction practices for concrete pavement: a state of the practice manual. Concr. Pavem.

Trauchessec, R., Mechling, J.M., et al., 2015. Hydration of ordinary Portland cement and calcium sulfoaluminate cement blends. Cem. Concr. Comp. 56, 106-114. https://doi.org/10.1016/j.cemconcomp.2014.11.005

Volder, A., Watson, T., Viswanathan, B., 2009. Potential use of pervious concrete for maintaining existing mature trees during and after urban development. Urban For. & Urban Gree. 8(4), 249-256. https://doi.org/10.1016/j.ufug.2009.08.006

Yan, X., Gong, C., Wang, S., et al., 2013. Effect of aggregate coating thickness on pore structure features and properties of porous ecological concrete. Mag. Concr. Res. 65 (1), 1-8. https://doi.org/10.1680/macr.12.00234

Zhang, J., Taylor, P., Shi, C., 2015. Investigation of approaches for improving the interfacial transition zone related freezing and thawing resistance in concrete pavements. ACI Mater. J. http://dx.doi.org/10.14359/51687902

TABLES

Table 1

Chemical compositions of SAC (wt. %)

Oxide	SiO_2	CaO	Al_2O_3	Fe_2O_3	MgO	K_2O	Na_2O	TiO_2	SO_3	Los
Result	9.60	45.16	21.64	2.45	1.28	1.38	0.17	1.03	10.73	6.35

Table 2

QXRD data of SAC (%)

Mineral	$C_4A_3\$$	C_2S	C_3S	C_4AF	$C\$H_2$	C$	$CaCO_3$
Result	42.7	19.7	13.4	5.36	2.9	2.7	13.26

Table 3

Physical properties of crushed concrete aggregates in comparison to commercial aggregates

Aggregate type	Natural aggregate	Recycled aggregate
Gradation (mm)	20-25	20-25
Crush index (%)	9.3	18.3
Density (kg/m^3)	2730	2590
Water absorption (%)	0.6	5.6
Water absorption for 5 min (%)	0.6	3.3
Unit weight (kg/m^3)	1590	1320
Absolute volume (%)	58.5	51.6

Table 4

Mix proportion and preparation method of planting concrete

Sample	Unit weight (kg/m^3)					Mixing	Consolidating	Time/s	Pressure/MPa
Name	SAC	Aggregate	water	BA	PP	procedure	method		
Aref	220	1320	55	0.87	2.39	A	-	-	-
AV1							V	5	-
AV2								10	-
AV3								15	-
AV4								20	-
AV5								25	-
AP1							P	-	0.5
AP2								-	1.0
AP3								-	2.0
AR							R	-	-
BV3						B	V	a	-
BP2							P	-	b
BR							R	-	-
CV3						C	V	a	-
CP2							P	-	b
CR							R	-	-

a: 15 seconds optimum vibrating time; b: 1.0 MPa optimum consolidation pressure.

Table 5

Raw materials mixing methods for preparing planting concrete

Method A	Method B	Method C
1) Recycled aggregates and water were mixed together in a concrete mixer for 30 seconds; 2) SAC was slowly added into the mixture in 60 seconds; 3) The fresh mixture was further mixed for another 60 seconds..	1) Recycled aggregates were soaked in water until the weight maintained no more than 0.5 %; 2) Kept the recycled aggregates in a saturated-surface dry (*SSD*) condition; 3) SSD recycled aggregates and half of SAC were mixed in a concrete mixer for 30 seconds; 4) The left SAC and water were added into the mixture above with	1) Recycled aggregates and half of water were mixed for 30 seconds in a concrete mixer. 2) Half of SAC was added and mixed for another 60 seconds. 3) Left water and SAC were added into the mixture above with further mixing of 120 seconds.

further mixing of 120 seconds.

Table 6

Mix proportions of planting concrete with fertilizer (kg/m^3)

Sample Name	Aggregate type		SAC	Water	Urea	DP	BA	PP
	Recycled	Natural						
N	-	1590	265	66	-	-	1.06	2.92
Rref	1320	-	220	55	-	-	0.87	2.39
RU1		-			0.44	-		
RU2		-			4.4	-		
RU3		-			7.7	-		
RD1		-			-	0.44		
RD2		-			-	4.4		
RD3		-			-	7.7		

FIGURES

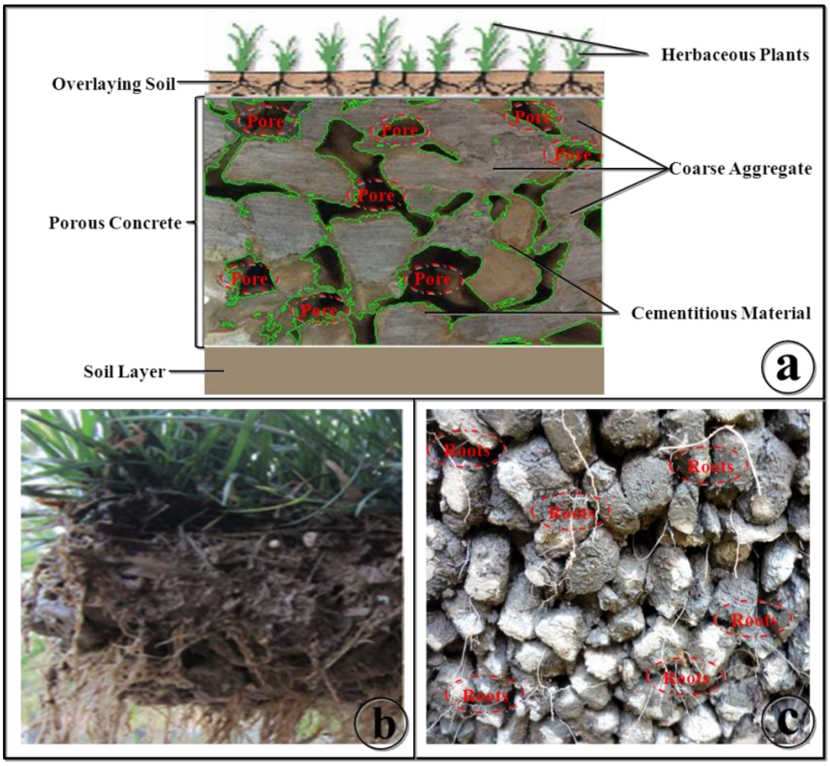

Fig.1 (a) Sketch map of planting concrete; (b) Actual-effect pictures of planting concrete; (c) Actual- effect pictures of plants' roots through the concrete.

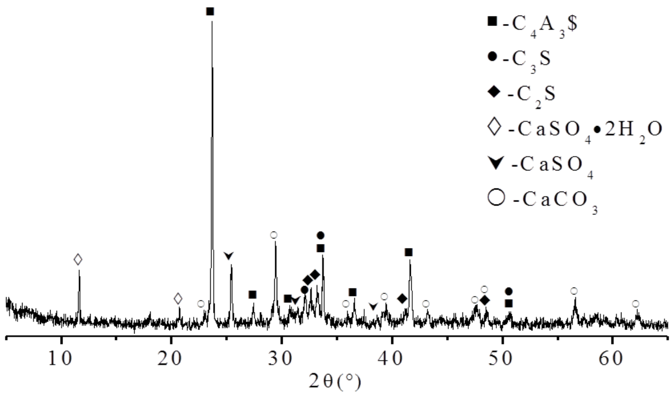

Fig. 2 X-ray analysis result of SAC.

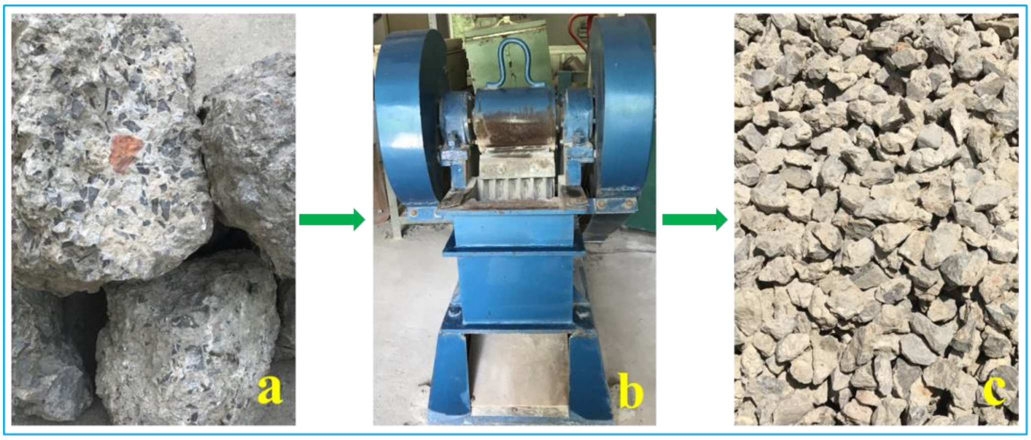

Fig. 3 The preparation process of recycled aggregates showing (a) the waste demolition concrete (b) the jaw crusher (c) the final crushed demolition concrete as aggregates

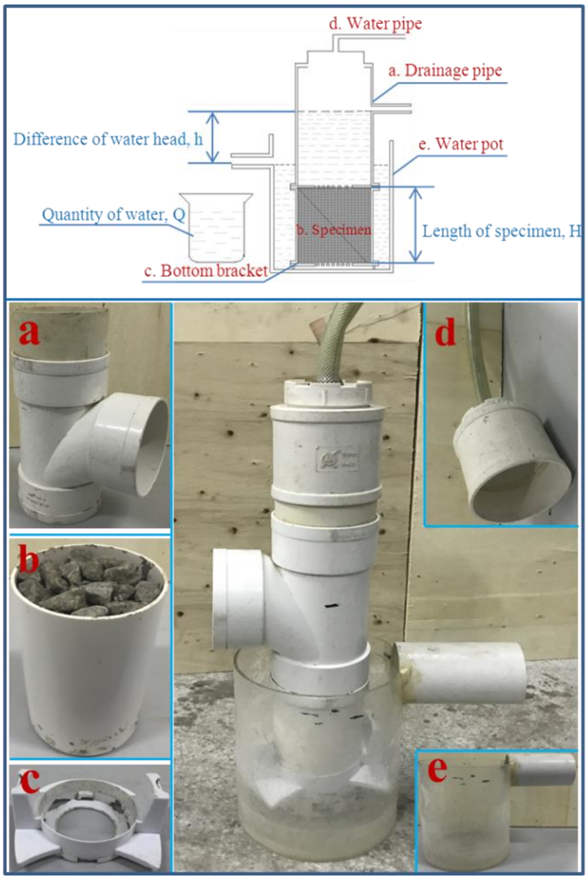

Fig. 4 CWP set-up for planting concrete.

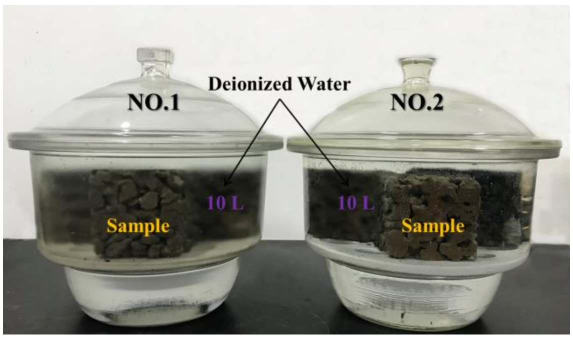

Fig. 5 Pictures of the test of fertilizer release rate and alkalinity of pore fluid.

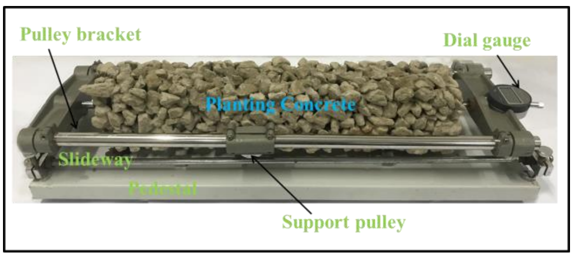

Fig. 6 Drying shrinkage test set-up of planting concrete.

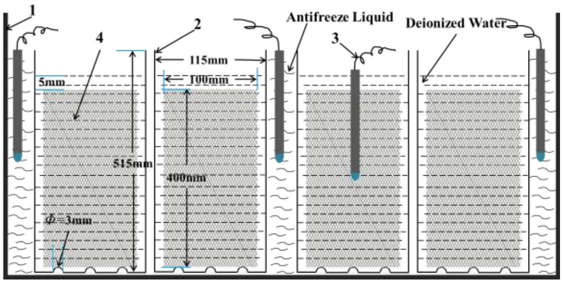

Fig.7 Schematic view of frost resistance test. 1, Freeze-thawing cycle machine; 2, Rubber container (115 mm × 115 mm × 515 mm); 3, Temperature Sensor; 4, Sample (100 mm × 100 mm × 400 mm).

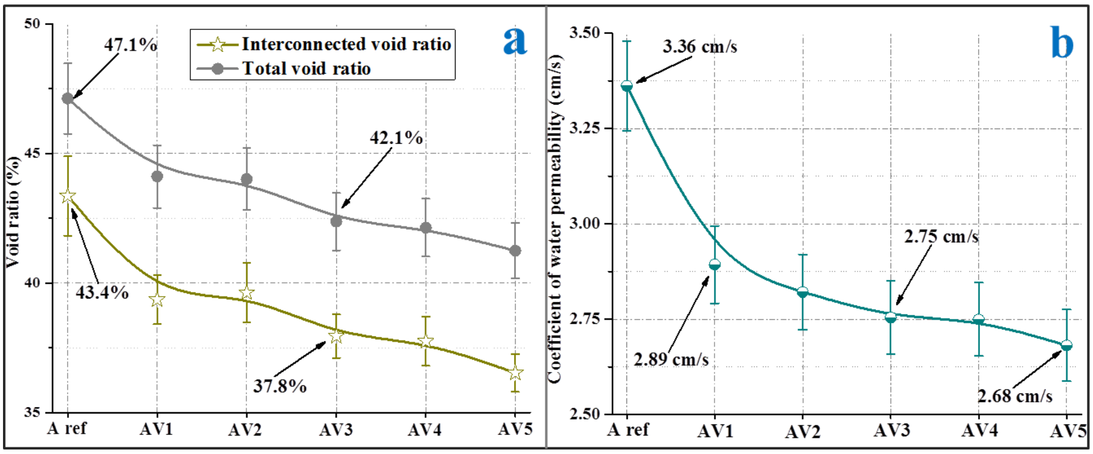

Fig. 8 (a) Void ratio and (b) CWP of planting concrete (consolidated by vibration).

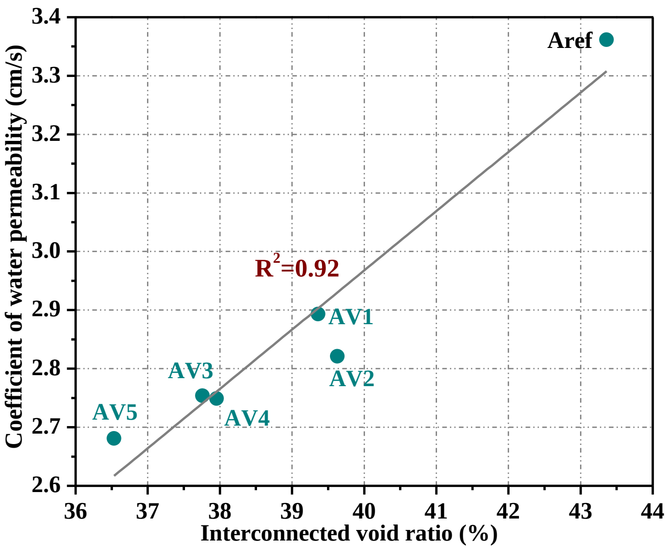

Fig. 9 Relationship between interconnected void ratio and CWP of planting concrete (consolidated by vibration).

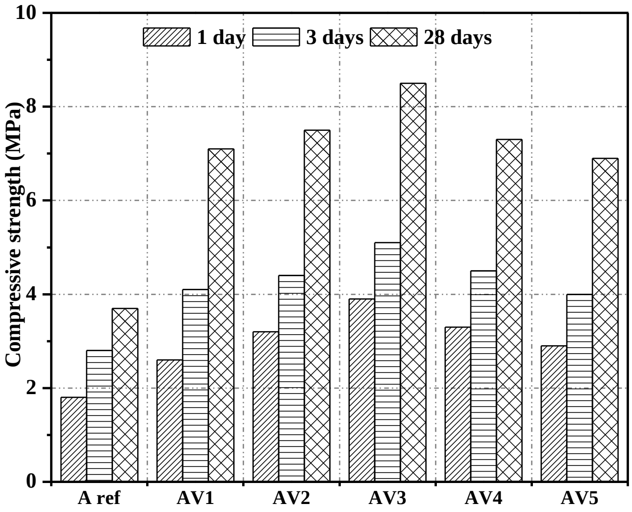

Fig. 10 Compressive strength of planting concrete (consolidated by vibration).

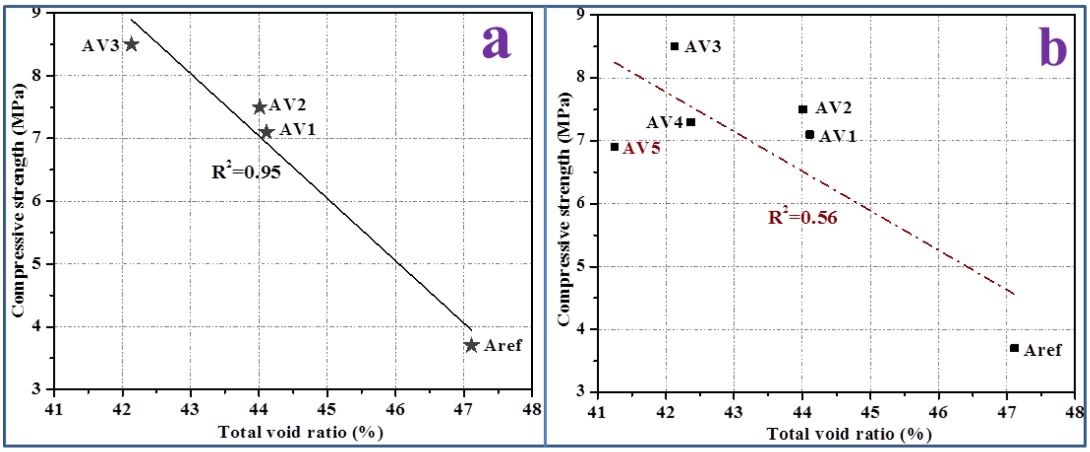

Fig.11 Relationship between total void ratio and 28 days compressive strength of planting concrete (consolidated by vibration).

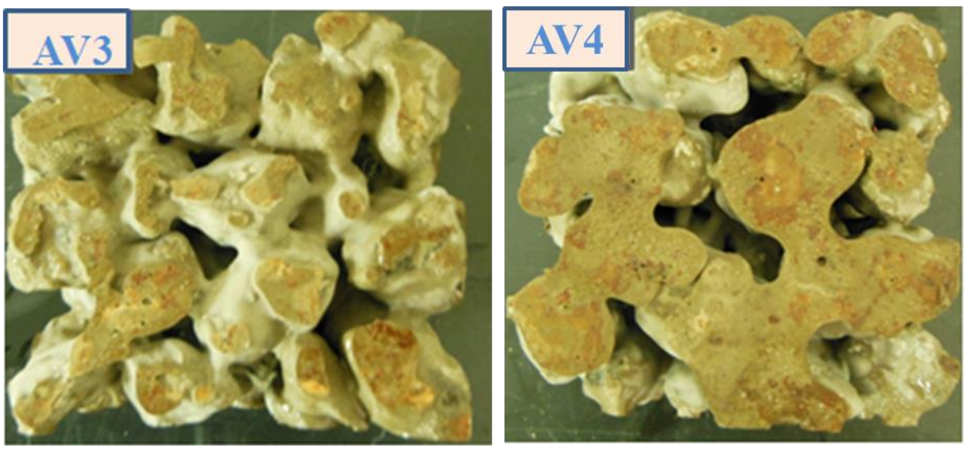

Fig. 12 Images of the bottom of (a) sample AV3 and (b) AV4 consolidated by vibration.

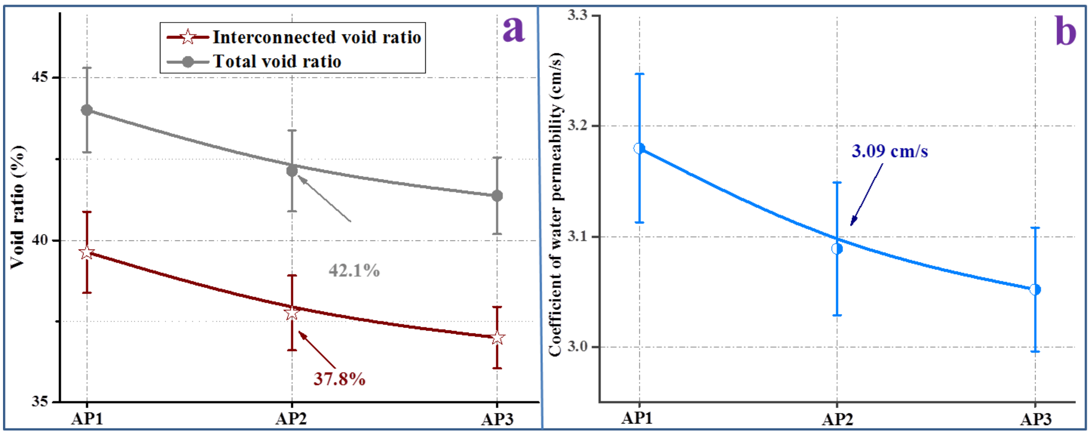

Fig. 13 (a) Total void and interconnected void ratio and (b) CWP of planting concrete (consolidated by pressure).

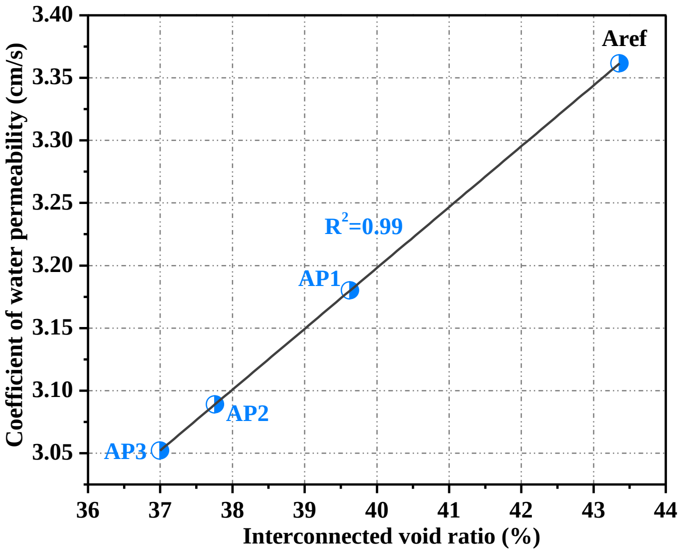

Fig. 14 Relationship between interconnected void ratio and CWP of planting concrete (consolidated by pressure).

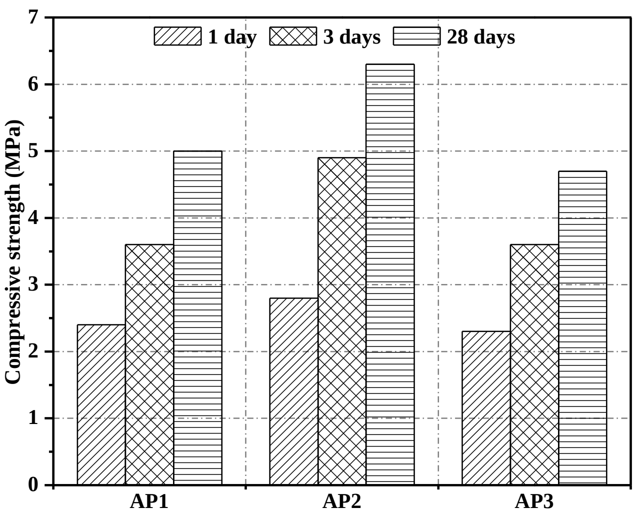

Fig. 15 Compressive strength of planting concrete (consolidated by pressure).

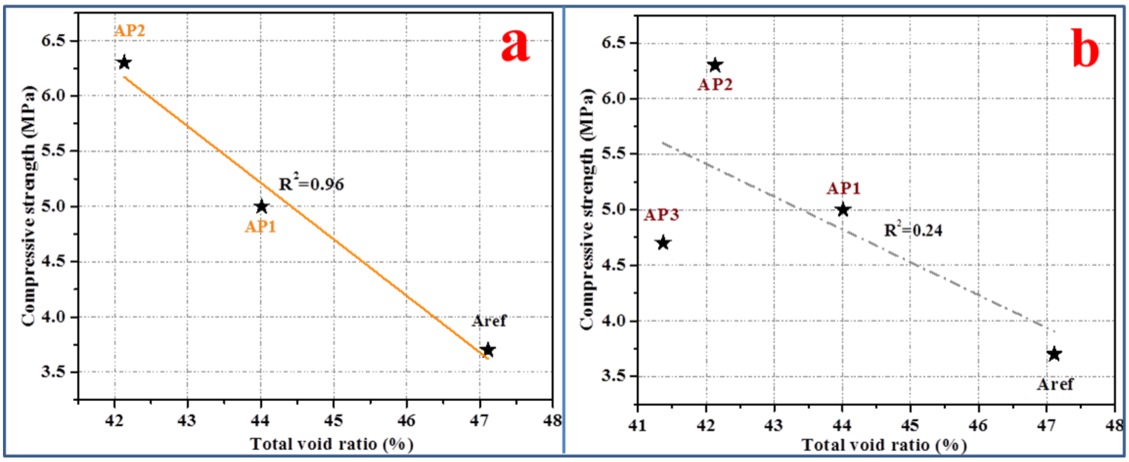

Fig. 16 Relationship between total void ratio and 28-day compressive strength of planting concrete (consolidated by pressure).

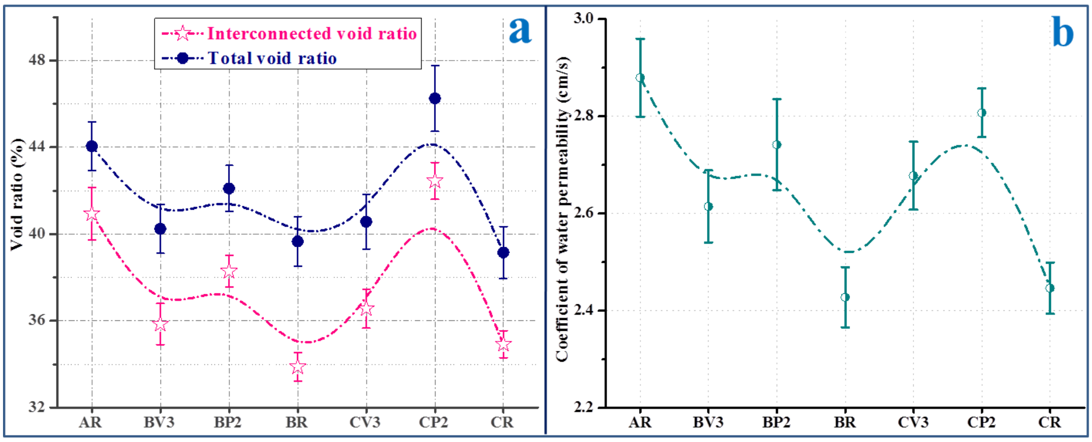

Fig. 17 (a) Total void and interconnected void ratio and (b) CWP of planting concrete.

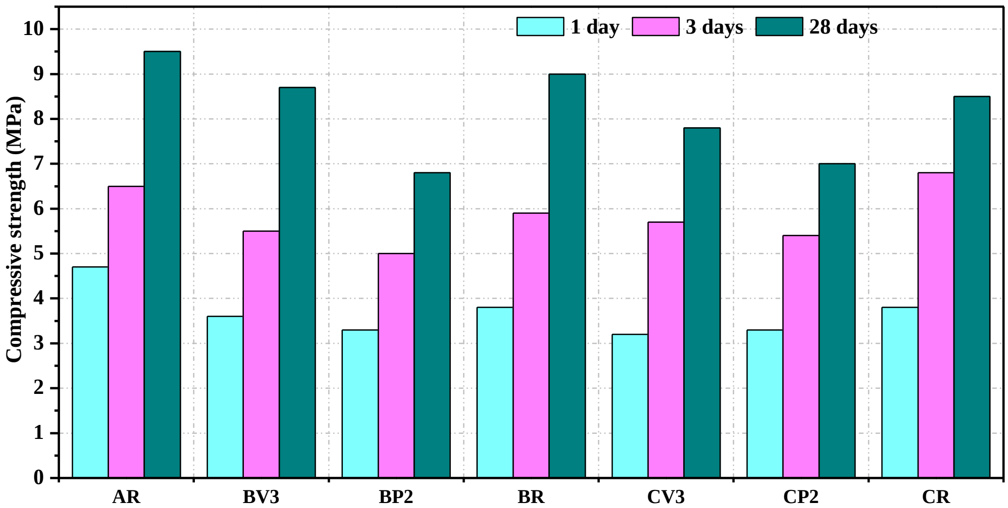

Fig. 18 Compressive strength of planting concrete.

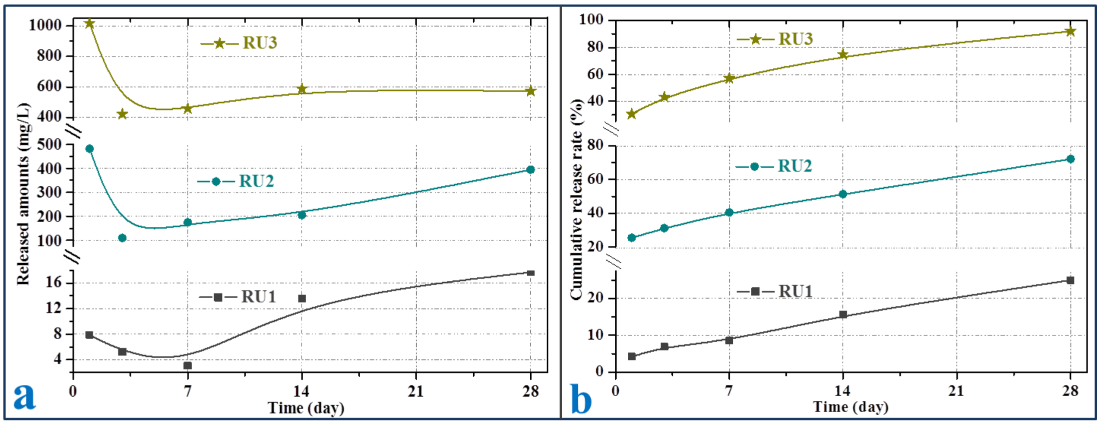

Fig. 19 Release amounts and cumulative release rates of nitrogen of planting concrete with urea.

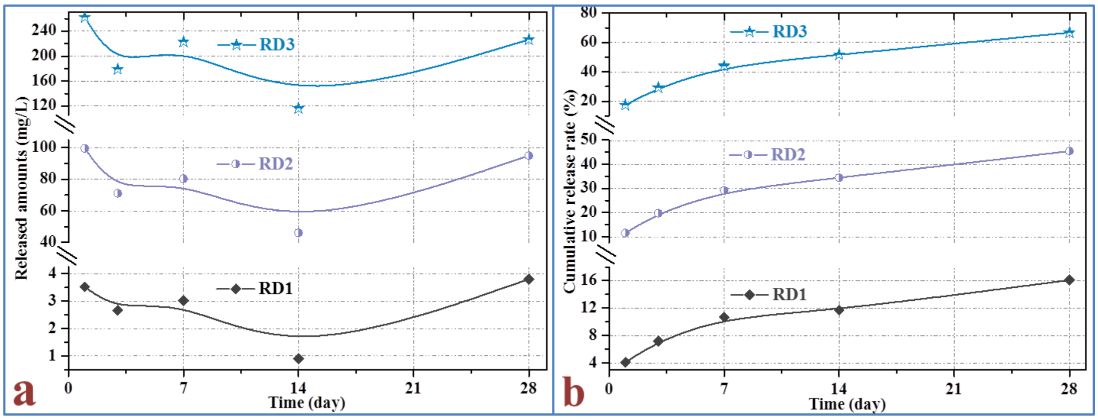

Fig. 20 Release amounts and cumulative release rate of nitrogen of planting concrete contains DP.

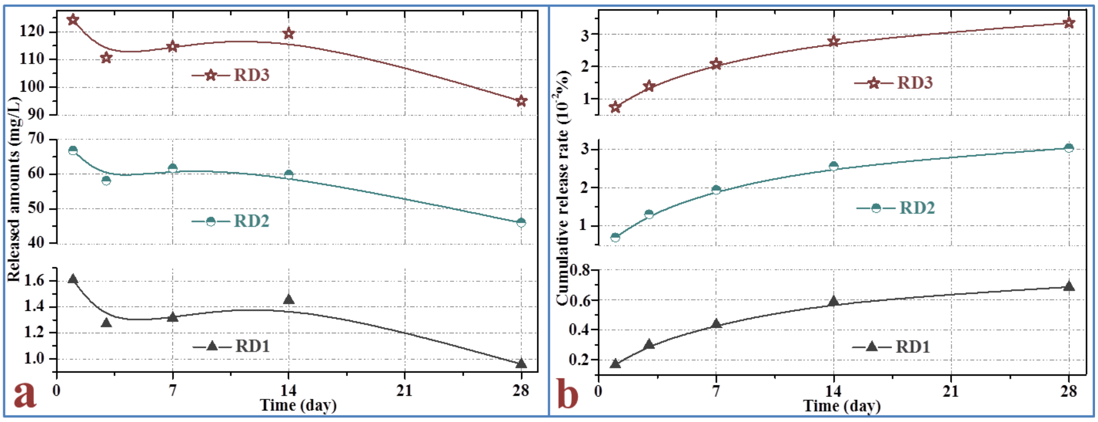

Fig. 21 Release amounts and cumulative release rate of phosphorus of planting concrete contains DP.

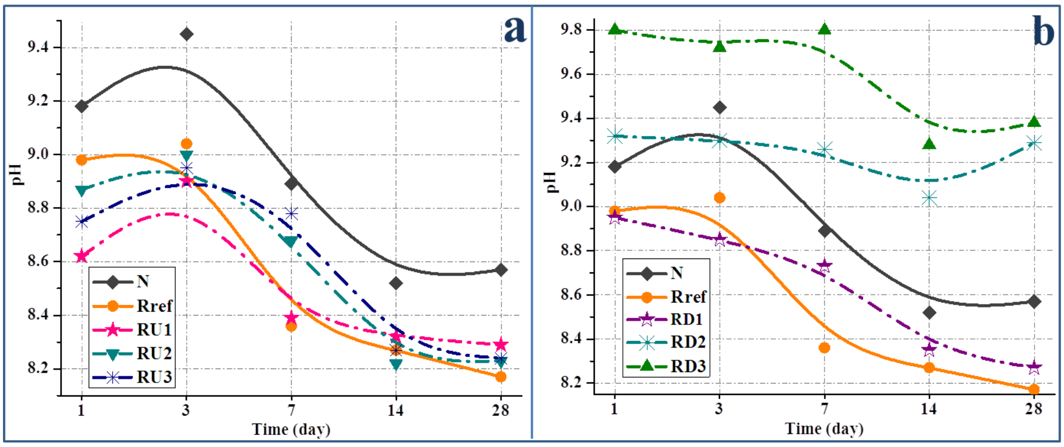

Fig. 22 Alkalinity of pore fluid of planting concrete at various ages.

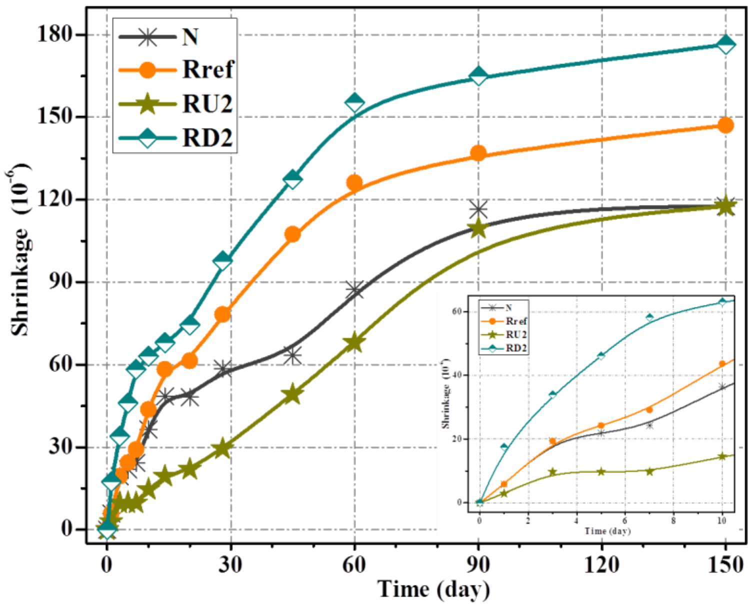

Fig. 23 Dry shrinkage of planting concrete at various ages.

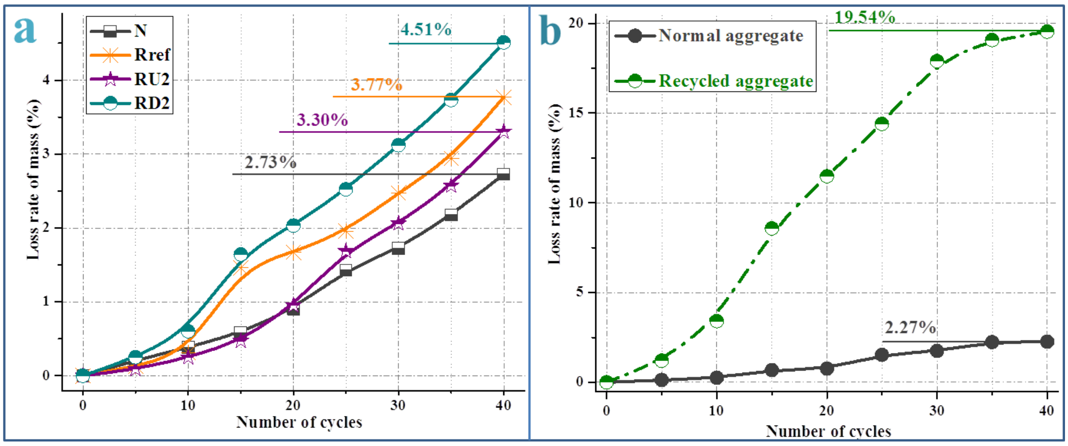

Fig. 24 Frost resistance (i.e. in terms of mass loss) of planting concrete.